

Provided for non-commercial research and education use.  
Not for reproduction, distribution or commercial use.



This article appeared in a journal published by Elsevier. The attached copy is furnished to the author for internal non-commercial research and education use, including for instruction at the authors institution and sharing with colleagues.

Other uses, including reproduction and distribution, or selling or licensing copies, or posting to personal, institutional or third party websites are prohibited.

In most cases authors are permitted to post their version of the article (e.g. in Word or Tex form) to their personal website or institutional repository. Authors requiring further information regarding Elsevier's archiving and manuscript policies are encouraged to visit:

<http://www.elsevier.com/copyright>



Contents lists available at ScienceDirect

Journal of Biomechanics

journal homepage: [www.elsevier.com/locate/jbiomech](http://www.elsevier.com/locate/jbiomech)  
[www.JBiomech.com](http://www.JBiomech.com)

## Biaxial mechanical testing of human sclera

Armin Eilaghi<sup>a,b</sup>, John G. Flanagan<sup>c,d</sup>, Inka Tertinegg<sup>c</sup>, Craig A. Simmons<sup>a,b</sup>,  
G. Wayne Brodland<sup>e,f</sup>, C. Ross Ethier<sup>a,b,c,g,\*</sup>

<sup>a</sup> Department of Mechanical and Industrial Engineering, University of Toronto, Canada

<sup>b</sup> Institute for Biomaterials and Biomedical Engineering, University of Toronto, Canada

<sup>c</sup> Department of Ophthalmology and Vision Sciences, University of Toronto, Canada

<sup>d</sup> Optometry School, University of Waterloo, Canada

<sup>e</sup> Department of Civil and Environmental Engineering, University of Waterloo, Canada

<sup>f</sup> Department of Biology, University of Waterloo, Canada

<sup>g</sup> Department of Bioengineering, Imperial College London, UK

### ARTICLE INFO

#### Article history:

Accepted 24 February 2010

#### Keywords:

Biaxial testing

Sclera

Stiffness

Tissue mechanical properties

Glaucoma

### ABSTRACT

The biomechanical environment of the optic nerve head (ONH), of interest in glaucoma, is strongly affected by the biomechanical properties of sclera. However, there is a paucity of information about the variation of scleral mechanical properties within eyes and between individuals. We thus used biaxial testing to measure scleral stiffness in human eyes. Ten eyes from 5 human donors (age  $55.4 \pm 3.5$  years; mean  $\pm$  SD) were obtained within 24 h of death. Square scleral samples (6 mm on a side) were cut from each ocular quadrant 3–9 mm from the ONH centre and were mechanically tested using a biaxial extensional tissue tester (BioTester 5000, CellScale Biomaterials Testing, Waterloo). Stress–strain data in the latitudinal (toward the poles) and longitudinal (circumferential) directions, here referred to as directions 1 and 2, were fit to the four-parameter Fung constitutive equation  $W=c(e^Q-1)$ , where  $Q=c_1E_{11}^2+c_2E_{22}^2+2c_3E_{11}E_{22}$  and  $W$ ,  $c$ 's and  $E_{ij}$  are the strain energy function, material parameters and Green strains, respectively. Fitted material parameters were compared between samples. The parameter  $c_3$  ranged from  $10^{-7}$  to  $10^{-8}$ , but did not contribute significantly to the accuracy of the fitting and was thus fixed at  $10^{-7}$ . The products  $c*c_1$  and  $c*c_2$ , measures of stiffness in the 1 and 2 directions, were  $2.9 \pm 2.0$  and  $2.8 \pm 1.9$  MPa, respectively, and were not significantly different (two-sided  $t$ -test;  $p=0.795$ ). The level of anisotropy (ratio of stiffness in orthogonal directions) was  $1.065 \pm 0.33$ . No statistically significant correlations between sample thickness and stiffness were found (correlation coefficients =  $-0.026$  and  $-0.058$  in directions 1 and 2, respectively). Human sclera showed heterogeneous, near-isotropic, nonlinear mechanical properties over the scale of our samples.

© 2010 Elsevier Ltd. All rights reserved.

### 1. Introduction

Glaucoma is a group of potentially blinding ocular diseases characterized by gradual and progressive damage to retinal ganglion cell axons forming the optic nerve (Fig. 1), and is usually associated with elevated intraocular pressure (IOP) (Allingham and Shields, 2005). Retinal ganglion cell damage occurs at the optic nerve head (ONH), where the optic nerve axons leave the eye posteriorly (Drance, 1995). A significant body of circumstantial evidence implicates biomechanical factors as playing a role in retinal ganglion cell damage in glaucoma (Burgoyne et al., 2005), but the precise damage mechanism remains unknown. For these reasons, it is important to

understand the biomechanics of the ONH. This is not straightforward due to the complex anatomy of the ONH, the fact that the constituent tissues have substantially different mechanical properties and the considerable inter-individual variability in the geometry of this region (Burgoyne et al., 2005; Drance, 1995).

Numerical modeling has been used to improve our understanding of ONH biomechanics (Bellezza et al., 2000; Sigal et al., 2004). A numerical sensitivity analysis showed that scleral stiffness strongly affects the biomechanics of ONH, being ranked first amongst 21 geometric and material properties that were considered in the analysis (Sigal et al., 2005). There is thus considerable motivation for characterizing the mechanical properties of sclera (Downs et al., 2008; Ethier, 2006).

The stiffness of human sclera is determined by the content and architecture of its structural proteins, primarily collagen (Schultz et al., 2008). Collagen fibers constitute approximately 90% of the dry weight of the sclera (Watson and Young, 2004), forming

\* Corresponding author at: Department of Bioengineering, Imperial College, London SW7 2AZ, UK. Tel.: +44 0 20 7594 9795; fax: +44 0 20 7594 9787.

E-mail address: [r.ethier@imperial.ac.uk](mailto:r.ethier@imperial.ac.uk) (C. Ross Ethier).

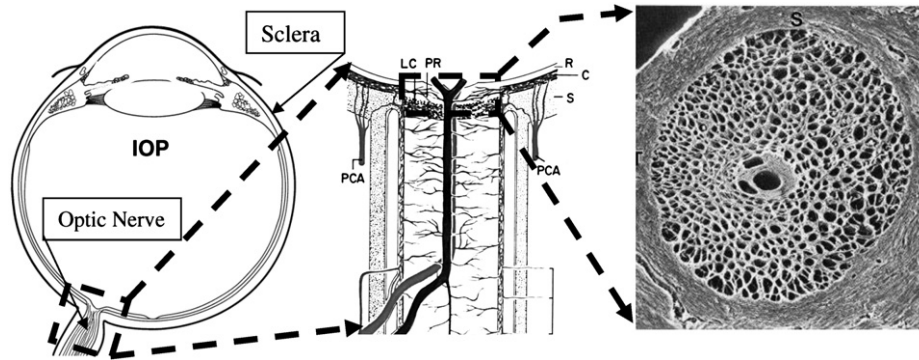


**Fig. 1.** Left panel: cross-sectional overview through a human eye. The boxed region is the optic nerve head area, and is shown magnified in the middle panel. Middle panel: overview of the major anatomical features of the optic nerve head. Symbols: LC—lamina cribrosa; PCA—posterior ciliary arteries; C—choroid; R—retina; S—sclera (Hayreh, 1975). Right panel: en face view of the lamina cribrosa, showing connective tissue elements only (Minckler, 1989). The pores, through which the nerve fibres pass, can be clearly seen.

**Table 1**

Values reported in the literature for the stiffness of human sclera, and methodologies used to obtain these values.

Source	Testing method	Pretension (MPa)	Max. strain(%)	Elastic modulus (MPa)
Woo et al. (1972)	Pressurization of the eye globe	$3 \times 10^{-4}$	13	2.3
Friberg and Lace (1988)	Uniaxial testing	$\sim 0.005$	Until rupture ( $\sim 20$ )	$2.9 \pm 1.4$
Battaglioli and Kamm (1984)	Unconfined compression	$2 \times 10^{-4}$	15	$2.7\text{--}4.1 \times 10^{-2}$
Wollensak and Spoerl (2004)	Uniaxial testing	0.01	10–15	22.82 (at 8% strain)

parallel bundles of different diameters (Summers Rada et al., 2006) that are organized in irregular interwoven layers (Komai and Ushiki, 1991). Previous histological studies have shown that a dominant scleral fiber alignment direction can only be identified in a few places, namely the peripapillary sclera (immediately adjacent to the ONH) and close to the extra-ocular muscle attachments (Thale and Tillmann, 1993; Thale et al., 1996), while fiber micro-architecture in the remainder of the sclera (which includes the locations of our samples) is described as random (Komai and Ushiki, 1991; Pinsky et al., 2005).

Previous studies of human sclera report widely varying mechanical properties (Table 1). This variability is likely due to differences in sample preparation and test protocols. For example, two of the tests used different levels of uniaxial loading (Friberg and Lace, 1988; Wollensak and Spoerl, 2004), one used pressurization of the eye globe (Woo et al., 1972) and the other unconfined compression (Battaglioli and Kamm, 1984).

In this study, we measured the stress–strain response of scleral samples taken from different locations in human eyes, using donors of approximately the same age and using a physiologically reasonable level of stress. Our aim was to investigate scleral nonlinearity and anisotropy, and variations within an eye, between eyes from a single individual and between individuals.

**2. Materials and methods**

Ten eyes from five human donors (age  $55.4 \pm 3.5$  years, mean  $\pm$  standard deviation) were obtained from the Eye Bank of Canada (Ontario Division, Toronto, Ontario). Eyes were free of known disease. All eyes were obtained within 24 h of death. The eyes were stored in normal saline at 4 °C until use. Each eye was prepared by surgically removing the internal ocular structures to leave only a scleral shell.

This shell was mounted on an appropriately sized sphere on the end of a post and cut into 6 mm  $\times$  6 mm segments with a custom-made cutting tool that included two parallel razor blades. The dissection and testing were done within 72 h postmortem, over which time scleral mechanical properties are known to

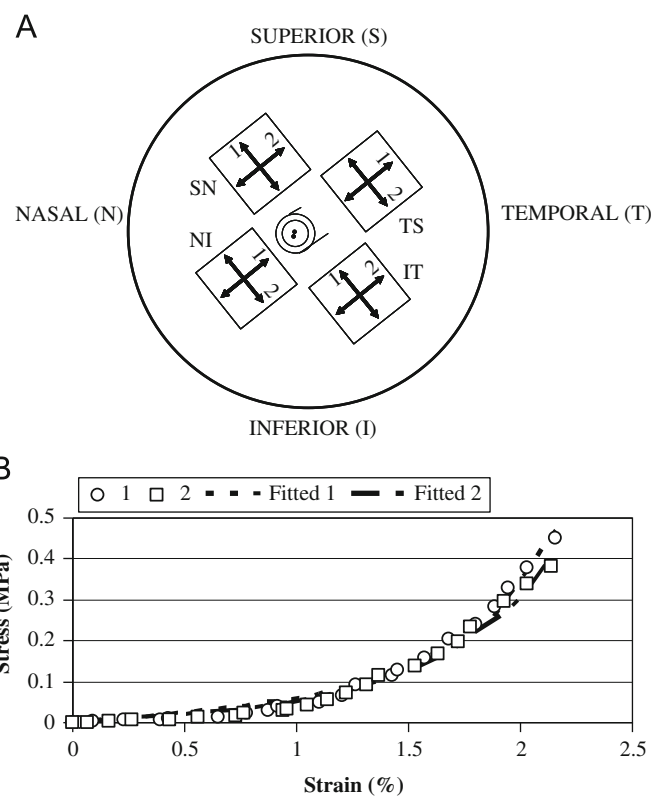


**Fig. 2.** (A) A schematic posterior view of a right eye showing locations of the four scleral samples taken from each eye in the temporal-superior (TS), superior-nasal (SN), nasal-inferior (NI) and inferior-temporal (IT) directions. The samples were stretched in the polar (1) and circumferential (2) directions (T=Temporal, N=Nasal, S=Superior meridian and I=Inferior). (B) A typical stress–strain relationship for a sample in directions 1 and 2 consistent with panel A (data points) and the fitted Fung strain energy model (dashed lines).

**Table 2**  
Information for the human eyes used in this research. The running order of experiments for each eye was TS, SN, NI, IT. For more detailed information about the sample preparation and nomenclature of locations (i.e. quadrants), see Fig. 2. OD=right eye, OS=left eye.

Donor number	Eye number	OD or OS	Age (year)	Gender	Postmortem time to enucleation (h)	Postmortem time to testing (h)
1	75620	OD	57	Male	8	22
1	75621	OS	57	Male	8	20
2	75524	OD	59	Male	2	28
2	75525	OS	59	Male	2	26
3	76316	OD	50	Female	3	35
3	76317	OS	50	Female	3	37
4	76940	OD	54	Female	7	43
4	76941	OS	54	Female	7	45
5	75836	OD	57	Male	13	17
5	75837	OS	57	Male	13	20

remain constant (Girard et al., 2007). The samples were marked with tissue ink to keep track of their orientation during the experiments. Four samples were harvested from the meridians extending from the centre of the ONH in the temporal-superior, superior-nasal, nasal-inferior and inferior-temporal directions (panel A in Fig. 2) at distances of 3–9 mm from the centre of the ONH. These samples were designated “TS”, “SN”, “NI” and “IT”, respectively (T=temporal, N=na-sal, S=superior and I=inferior). The sample location and orientation were chosen to avoid the effect of muscle attachments (e.g. temporal oblique), since there is evidence that scleral microstructure is affected in the regions where muscles attach to the globe (Thale and Tillmann, 1993).

After dissection, each sclera sample was kept in normal saline supplemented with 100 U/ml penicillin, 100 µg/ml streptomycin and 5% serum until testing. Time for testing was from 15 min to 2 h. Sclera can be stored up to 72 h without mechanical deterioration (Girard et al., 2007), and we therefore tested our samples within 45 h postmortem (Table 2).

Samples were mounted in a biaxial tissue tester (BioTester 5000, CellScape Biomaterials Testing, Waterloo, Canada), equipped with load cells having an accuracy of 5 mN. The choice of a biaxial testing approach was based on estimates of the in vivo biomechanical environment of the sclera. According to the criterion often applied to define a thin shell, the ratio of the thickness (*t*) to radius of curvature (*r*) (i.e. eye globe radius) should be small ( $t/2r \ll 1$ ). In the case of the eye globe this criterion is fulfilled, since  $t/2r$  is 0.02–0.04. In this situation the in-plane stress is very much larger than the bending stress. It may be concluded that the applied load is resisted primarily by the in-plane stressing of the shell (Ugural 2003). The sizes of samples were also small with the gauge length of testing being 4.5 mm.

The samples were mounted in the tissue tester using a set of four BioRakes, each consisting of five tines (thin tungsten wires) used to anchor one edge of the specimen ( ). The details of the experimental approach are described in Eilaghi et al. (2009). In brief, loads were applied to small square samples (gauge length=4.5 mm) using a system of tines, and the resulting deformations were optically measured in the centre of the sample to avoid mechanical interference with the specimen, consistent with Humphrey et al. (1987, 2002). Samples were preloaded from a relaxed state to 20 mN to provide full contact between the tines and the specimen and to ensure that the sample was flattened and were preconditioned following the protocol of Downs et al. (2003). After being submerged in 37 °C isotonic saline, the specimen was subjected to a preconditioning protocol (Fig. 3) followed by displacement-controlled cycles to measure its stress–strain characteristics. Optical strain measurements were conducted through particle tracking of artificial markers adhered to the centre of the sample’s surface (Eilaghi et al., 2009) using particle tracking software provided with the BioTester. The spatial resolution of the optical system was ~ 1 µm. The thickness of each sample was measured after the test using a friction micrometer with an accuracy of 5 µm.

Since a controlled-displacement approach was used, the maximum applied stress varied between samples, with an average maximum applied stress for all samples being about 0.3 MPa. This value was an upper bound for scleral stresses under physiologic and pathophysiologic (glaucomatous) conditions, computed from Laplace’s law for a globe radius of 12 mm, scleral thickness of 0.5 mm and IOP of 187.5 mmHg.

The forces from the load cells in two directions were used to calculate the Kirchoff stresses. The resultant stress–strain data was then fit to the 4 parameter Fung constitutive model (Fung, 1993):

$$W = c(e^Q - 1), \quad Q = c_1 E_{11}^2 + c_2 E_{22}^2 + 2c_3 E_{11} E_{22} \quad (1)$$

$$S_{ij} = \frac{\partial W}{\partial E_{ij}} \quad (2)$$

where *W*, *c*’s, *E<sub>ij</sub>* and *S<sub>ij</sub>* are the Fung strain energy function, material parameters, Green strains and Kirchoff stresses, respectively. Best-fit values of the material parameters were found using nonlinear regression (Levenberg–Marquardt algo-

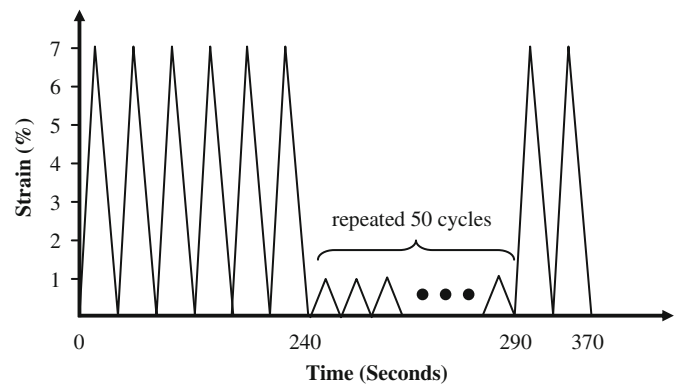


**Fig. 3.** The preconditioning protocol included six cycles of 7% equi-biaxial stretch, followed by 50 cycles of 1% equi-biaxial stretch to mimic the ocular pulse. Immediately after preconditioning, the sample was preloaded to 20 mN and two measurement cycles were conducted to ensure that the sample was preconditioned well (i.e. the mechanical response was repeatable over measurement cycles). Note that strains in the preconditioning phase were nominal values based on the movement of the actuators and thus likely overestimate the actual strain delivered to the central sample (Eilaghi et al., January, 2009). The movements of markers located on the central tissue sample were used to calculate strains in the rest of the study.

ri-thm with SIGMASTAT 3.5, Systat Software Inc., San Jose, CA, USA). The initial guesses for the material parameters were varied over a range of 10<sup>6</sup> for each parameter to ensure the fitting parameters were global minima. The constraints *c*, *c*<sub>1</sub>, *c*<sub>2</sub>, *c*<sub>3</sub> > 0 and *c*<sub>1</sub>, *c*<sub>2</sub> > *c*<sub>3</sub> were used to ensure convexity of the regression results (David et al., 2007; Holzapfel et al., 2000; Humphrey, 1999) (panel B in Fig. 2).

Stress–strain data for 30 samples (seven IT, eight NI, nine SN, and six TS—consistent with Fig. 2) that were free of testing artifacts were included in the regression analysis. The regression gave values of the parameter *c*<sub>3</sub> that were always far less than other parameters (typically < 10<sup>−7</sup>) and did not contribute significantly to the fitting process. Therefore, *c*<sub>3</sub> was fixed at 10<sup>−7</sup> and the regression was repeated. The fitting error increased no more than 0.7% as a result of fixing *c*<sub>3</sub>, confirming its insignificant contribution to the fitting process for our data set. This simplified the physical interpretations of the other parameters in the Fung exponential model. To ensure that the material parameters were not sensitive to the initial guesses we did regression tests starting with different initial guesses for *c*, *c*<sub>1</sub> and *c*<sub>2</sub>, in which initial guesses varied by up to 6 orders of magnitude, i.e. up to 1000 times larger and smaller. The results were similar to those obtained with the original initial guesses, with maximum variation < 3% and in many cases exactly the same answer. We conclude that our results were not sensitive to the initial guesses. It is important to note that although these derived measures of stiffness are useful for testing hypotheses such as anisotropy and stiffness between samples, they should not be confused with elastic modulus.

For a material with Fung constitutive behaviour, the Kirchoff stress can be calculated from Eqs. (1) and (2) as

$$\begin{aligned} S_{11} &= c(c_1 E_{11} + 2c_3 E_{22})e^{(c_1 E_{11}^2 + c_2 E_{22}^2 + 2c_3 E_{11} E_{22})} \\ S_{22} &= c(c_2 E_{22} + 2c_3 E_{11})e^{(c_1 E_{11}^2 + c_2 E_{22}^2 + 2c_3 E_{11} E_{22})} \end{aligned} \quad (3)$$

Since the value of *c*<sub>3</sub> was fixed at 10<sup>−7</sup> and *E*<sub>11</sub> and *E*<sub>22</sub> are of the order of 10<sup>−2</sup>, the products *c*\**c*<sub>1</sub> and *c*\**c*<sub>2</sub> can be considered as measures of stiffness in directions 1 and 2, respectively.

Considering the above equations for an equi-biaxial test, the ratio of stresses in the orthogonal directions is

$$\frac{S_{11}}{S_{22}} = \frac{c_1}{c_2} \quad (4)$$

Therefore, the ratio  $c_1/c_2$  was used as a measure of anisotropic response in the samples.

Five donors were used for this study. For each donor, both eyes (right and left) were studied. For each eye, samples were taken from four locations (IT, NI, SN and TS quadrants) and scleral stiffness was measured in two directions. In order to investigate the variation of stiffness amongst the samples we used a four-way ANOVA model that considered the following four factors: donor, right vs left eye, sample location and test direction. Further post-hoc three-way, two way and one-way ANOVAs were carried out by collapsing the non-significant variables.

### 3. Results

When averaged over all eyes and all samples, the stiffness products  $c \times c_1$  and  $c \times c_2$  were  $2.9 \pm 2.0$  MPa (mean  $\pm$  standard deviation) and  $2.8 \pm 1.9$  MPa, respectively. The stress–strain graph of the 30 samples tested in this research is presented in Fig. 4 which provides an overview of the range of stiffness behaviour in the tested samples. The amount of shear experienced in the central region of the specimens was also studied in five randomly selected samples. Calculations showed that shear strain, expressed as a percent of the normal strain, was  $6.7 \pm 4.3$  percent in equi-biaxial stretching tests. Distributions in both directions showed normal (Gaussian) distributions, passing the Kolmogorov–Smirnov (K–S) normality test (K–S Dist.=0.11 and 0.15 in the 1 and 2 directions).

Four-way ANOVA indicated no statistically significant differences for scleral stiffness for all the main factors and interactions ( $p \gg 0.05$ ). Similarly, collapsing the data for non-significant variables and analysing post-hoc ANOVA tests (three-way, two-way and one-way ANOVAs) did not show any statistically significant differences. However, it should be noted that the statistical power was small (0.05–0.07) so we cannot state with certainty that there was not a dependence of mechanical properties on the parameters, only that no significant difference was found.

The scleral samples showed no specific pattern of anisotropy in equi-biaxial tests, with a level of anisotropy (ratio of coefficients  $c_1/c_2$ ) of  $1.065 \pm 0.33$  (Fig. 5). The distribution of  $c_1/c_2$  was also

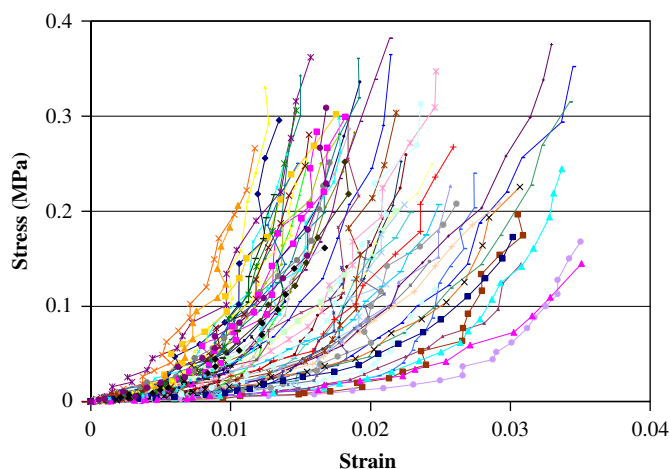


Fig. 4. The stress–strain data from the biaxial scleral tests (30 samples) to give an overall representation of the data. The small jags in the stress–strain graphs were non-physical and were related to optical strain measurement errors. The magnitude of the resulting error in strain was found to be generally  $< 0.0005$  and the effect of removing suspicious data points and redoing the regression analysis was  $< 6\%$  for the magnitudes of  $cc_1$  and  $cc_2$ . The raw stress–strain data that this graph is based on are provided as a supplemental data file.

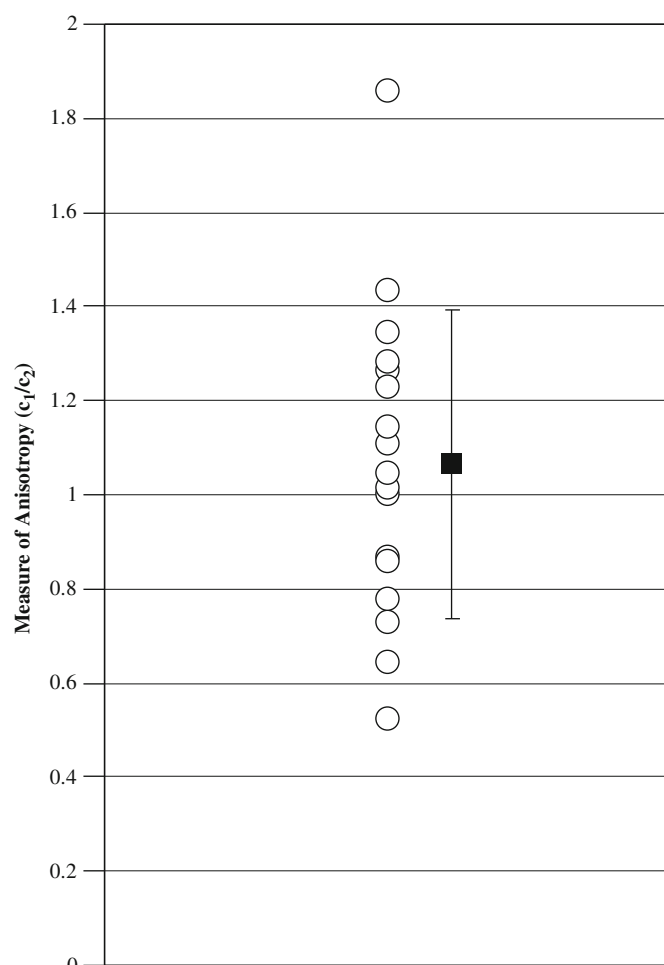


Fig. 5. The average anisotropic response of the samples, shown as a plot of the ratio  $c_1/c_2$ . All values are graphed as a point, with error bars on the right of the column. The scleral samples showed close-to-isotropic behaviour, with the ratio of stiffnesses being  $1.065 \pm 0.33$ .

normal (passed the K–S normality test, K–S Dist.=0.08). The maximum and minimum levels of anisotropy amongst the four locations occurred in the IT quadrant (1.17) and the NI quadrant (0.87), respectively. No statistically significant correlations were found between thickness and scleral stiffness in both directions (Fig. 6) with Pearson correlation coefficients of  $-0.026$  ( $p=0.89$ ) and  $-0.058$  ( $p=0.76$ ) in the polar (1) and circumferential (2) directions, respectively.

Grouping all the measurements from each individual (Fig. 7) showed the average scleral stiffness for the five individuals studied varied from 2.8 to 3.3 MPa and the intra-subject coefficient of variation was 15%. The inter-subject coefficients of variation were higher (49%, 84%, 68%, 63%, 64% for individuals 75620&21, 75524&25, 76316&17, 76340&41 and 75836&37).

### 4. Discussion

Our results show that the biomechanical properties of sclera are heterogeneous, nonlinear and isotropic. Previously, the non-linear mechanical response of sclera was noted (Woo et al., 1972), but an elastic modulus, which assumes linear (Friberg and Lace, 1988) or bi-linear (Kobayashi et al., 1971) elastic behaviour, was reported. Our work represents a more complete characterization of human scleral biomechanical properties. In our tests human

scleral samples showed nonlinear mechanical behaviour. We used a reduced form of Fung's exponential constitutive equation to characterize this behaviour, in which the products  $c_1c_2$  and  $c_1c_2$  can be used as measures of stiffness in orthogonal directions. Although these products are not strictly translatable into more conventional tangent modulus values, this approach allows for comparing the stiffness of samples and also for creating scleral

material models for computational modelling of optic nerve head biomechanics.

Our measures of stiffness ( $c_1c_2$  and  $c_1c_2$ ) were determined by biaxial loading, making samples appear stiffer than they would under uniaxial loading. For example, a linearly elastic and incompressible ( $\nu=0.5$ ) thin sample, when stretched equibiaxially shows an effective modulus of twice the elastic modulus. When the strains are very small the exponential component of the stress-strain relationship (Eq. (3)) becomes very close to unity and therefore our results suggest an average low strain linear biaxial modulus of 2.8–2.9 MPa, which is slightly less but still comparable with the elastic modulus values reported by Woo et al. (1972) and Friberg and Luce, (1988) (see Table 1 and note the  $2 \times$  biaxial effect). However, our results suggest a significantly less stiff behaviour for sclera than previously reported by Spoerl et al. (2005). The discrepancy may arise because our tests loaded the sclera to a nominal stress of 0.3 MPa, whereas the latter studies used a maximum stress  $> 3$  MPa, a value perhaps more relevant to traumatic ocular injuries.

Finally, we saw no specific pattern of anisotropy in the stiffness of scleral samples (Figs. 4 and 5). Specifically, no statistically significant differences were found between the directional stiffnesses of scleral samples ( $p=0.795$ ). However, this may be a statistical power issue; considering our sample sizes and standard deviations, a power analysis indicated that we would only be able to detect a difference of 1.4 MPa in means between the two directions for a power of 0.8 with significance criterion  $\alpha=0.05$ . Nonetheless, the apparent isotropy may be related to the random orientation of collagen bundles in the human sclera away from the optic nerve head insertion and muscle attachments (Thale and Tillmann, 1993; Thale et al., 1996) consistent with our samples' locations. No statistical differences were found between the stiffnesses of scleral samples from different eyes (left and right) or from different locations of an eye in our data, although the low statistical power means that we cannot state with certainty that these stiffnesses were similar.

The current study did not measure viscoelastic properties of sclera because the time scale of glaucoma, the condition of particular interest here, is of the order of months to years, suggesting that viscoelastic properties may be less important than static elastic properties. Also the experimental measurements presented in this paper are limited to eyes from donors in their 6th decade with ostensibly normal (disease-free) eyes. Future work should study viscoelastic properties, effects of age and of glaucoma history on the mechanical properties of sclera.

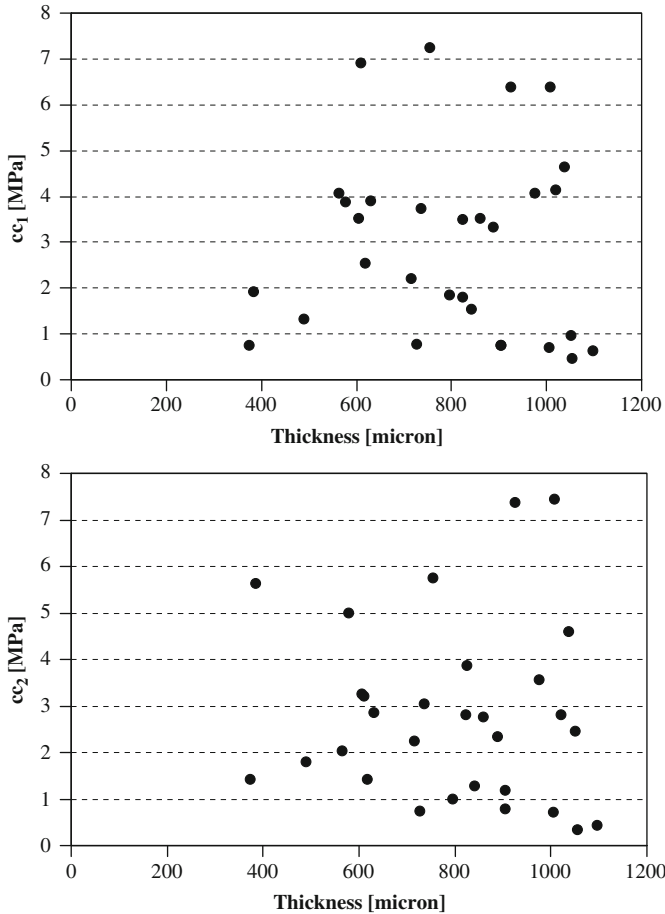


Fig. 6. Scatter-plots of scleral thickness versus measures of scleral stiffness. No statistically significant correlations were found between the thickness and the scleral stiffness in the polar (1) and circumferential (2) directions.

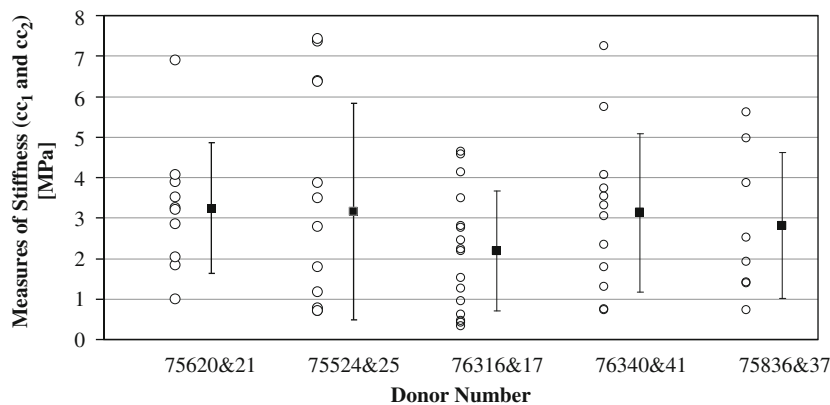


Fig. 7. Heterogeneity of scleral stiffness measured for different individuals. Each column includes measures of stiffness of both directions of all locations of the left and the right eyes of a pair. The numbers on the horizontal axis refer to individual donors.

## Conflict of interest

*Proprietary interest:* GW Brodland has an interest in CellScale Biomaterials Testing.

## Acknowledgments

We thank the donors' families and staff of the Canadian Eye Bank (Ontario Division) for donations of human eyes. Funding was provided through the Collaborative Health Research Project Program (CRE, GWB, JGF), Canadian Institutes of Health Research (JGF, CRE) and the Canada Research Chairs Program (CRE). We thank an anonymous reviewer for extensive comments and suggestions regarding the statistical analysis.

## Appendix A. Supplementary material

Supplementary data associated with this article can be found in the online version at doi:10.1016/j.jbiomech.2010.02.031.

## References

- Allingham, R.R., Shields, M.B., 2005. *Shields' Textbook of Glaucoma*. Lippincott Williams & Wilkins, Philadelphia.
- Battaglioli, J.L., Kamm, R.D., 1984. Measurements of the compressive properties of scleral tissue. *Investigative Ophthalmology and Visual Science* 1, 59–65.
- Bellezza, A.J., Hart, R.T., Burgoyne, C.F., 2000. The optic nerve head as a biomechanical structure: initial finite element modeling. *Investigative Ophthalmology and Visual Science* 10, 2991–3000.
- Burgoyne, C.F., Downs, J.C., Bellezza, A.J., Suh, J.K., Hart, R.T., 2005. The optic nerve head as a biomechanical structure: a new paradigm for understanding the role of IOP-related stress and strain in the pathophysiology of glaucomatous optic nerve head damage. *Progress in Retinal and Eye Research* 1, 39–73.
- David, G., Pedrigi, R.M., Heistand, M.R., Humphrey, J.D., 2007. Regional multiaxial mechanical properties of the porcine anterior lens capsule. *Journal of Biomechanical Engineering* 1, 97–104.
- Downs, J.C., Roberts, M.D., Burgoyne, C.F., 2008. Mechanical environment of the optic nerve head in glaucoma. *Optometry and Vision Science* 6, 425–435.
- Downs, J.C., Suh, J.K., Thomas, K.A., Bellezza, A.J., Burgoyne, C.F., Hart, R.T., 2003. Viscoelastic characterization of peripapillary sclera: material properties by quadrant in rabbit and monkey eyes. *Journal of Biomechanical Engineering* 1, 124–131.
- Drance, S.M., 1995. *Optic Nerve in Glaucoma*. Kugler Publications, New York.
- Eilaghi, A., Flanagan, J.G., Brodland, G.W., Ethier, C.R., 2009. Strain uniformity in biaxial specimens is highly sensitive to attachment details. *ASME Journal of Biomechanical Engineering* 131(9), 091003-1–091003-7.
- Ethier, C.R., 2006. Scleral biomechanics and glaucoma—a connection? *Canadian Journal of Ophthalmology* 1, 9–14.
- Friberg, T.R., Lace, J.W., 1988. A comparison of the elastic properties of human choroid and sclera. *Experimental Eye Research* 3, 429–436.
- Fung, Y.C., 1993. *Biomechanics: Mechanical Properties of Living Tissues*. Springer-Verlag, New York.
- Girard, M., Suh, J.K., Hart, R.T., Burgoyne, C.F., Downs, J.C., 2007. Effects of storage time on the mechanical properties of rabbit peripapillary sclera after enucleation. *Current Eye Research* 5, 465–470.
- Hayreh, S.S., 1975. *Anterior Ischemic Optic Neuropathy*. Springer-Verlag, Berlin.
- Holzapfel, G.A., Gasser, T.C., Ogden, R.W., 2000. A new constitutive framework for arterial wall mechanics and a comparative study of material models. *Journal of Elasticity* 1–3, 1–48.
- Humphrey, J.D., 1999. An evaluation of pseudoelastic descriptors used in arterial mechanics. *Journal of Biomechanical Engineering* 2, 259–262.
- Humphrey, J.D., Vawter, D.L., Vito, R.P., 1987. Quantification of strains in biaxially tested soft tissues. *Journal of Biomechanics* 1, 59–65.
- Humphrey, J.D., 2002. *Cardiovascular Solid Mechanics: Cells, Tissues, and Organs*. Springer, New York.
- Kobayashi, A.S., Woo, S.L., Lawrence, C., Schlegel, W.A., 1971. Analysis of the corneo-scleral shell by the method of direct stiffness. *Journal of Biomechanics* 5, 323–330.
- Komai, Y., Ushiki, T., 1991. The three-dimensional organization of collagen fibrils in the human cornea and sclera. *Investigative Ophthalmology and Visual Science* 8, 2244–2258.
- Minckler, D.S., 1989. Histology of optic nerve damage in ocular hypertension and early glaucoma. *Survey of Ophthalmology (Suppl. April)*, 401–402.
- Pinsky, P.M., Van Der Heide, D., Chernyak, D., 2005. Computational modeling of mechanical anisotropy in the cornea and sclera. *Journal of Cataract and Refractive Surgery* 1, 136–145.
- Schultz, D.S., Lotz, J.C., Lee, S.M., Trinidad, M.L., Stewart, J.M., 2008. Structural factors that mediate scleral stiffness. *Investigative Ophthalmology and Visual Science* 10, 4232–4236.
- Sigal, I.A., Flanagan, J.G., Ethier, C.R., 2005. Factors influencing optic nerve head biomechanics. *Investigative Ophthalmology and Visual Science* 11, 4189–4199.
- Sigal, I.A., Flanagan, J.G., Tertinegg, I., Ethier, C.R., 2004. Finite element modeling of optic nerve head biomechanics. *Investigative Ophthalmology and Visual Science* 12, 4378–4387.
- Spoerl, E., Boehm, A.G., Pillunat, L.E., 2005. The influence of various substances on the biomechanical behavior of lamina cribrosa and peripapillary sclera. *Investigative Ophthalmology and Visual Science* 4, 1286–1290.
- Summers Rada, J.A., Shelton, S., Norton, T.T., 2006. The sclera and myopia. *Experimental Eye Research* 2, 185–200.
- Thale, A., Tillmann, B., 1993. The collagen architecture of the sclera—SEM and immunohistochemical studies. *Annals of Anatomy* 3, 215–220.
- Thale, A., Tillmann, B., Rochels, R., 1996. Scanning electron-microscopic studies of the collagen architecture of the human sclera—normal and pathological findings. *Ophthalmologica* 3, 137–141.
- Watson, P.G., Young, R.D., 2004. Scleral structure, organisation and disease. A review. *Experimental Eye Research* 3, 609–623.
- Wollensak, G., Spoerl, E., 2004. Collagen crosslinking of human and porcine sclera. *Journal of Cataract and Refractive Surgery* 3, 689–695.
- Woo, S.L., Kobayashi, A.S., Schlegel, W.A., Lawrence, C., 1972. Nonlinear material properties of intact cornea and sclera. *Experimental Eye Research* 1, 29–39.